Published in final edited form as:

FASEB J. 2022 December ; 36(12): e22629. doi:10.1096/fj.202200907RR.

β1 Integrin Monoclonal Antibody Treatment Ameliorates Cerebral Cavernous Malformations

Sara McCurdy[1,#], **Jenny Lin**[1], **Robert Shenkar**[2], **Thomas Moore**[2], **Rhonda Lightle**[2], **Eva Faurobert**[3], **Miguel-Alejandro Lopez-Ramirez**[1], **Issam Awad**[2], **Mark H. Ginsberg**[1]

[1]Department of Medicine, University of California San Diego, LA Jolla CA

[2]Department of Neurological Surgery, University of Chicago, Chicago IL

[3]Univ. Grenoble Alpes, CNRS 5309, Inserm 1209, Institute for Advanced Biosciences, Grenoble, France.

Abstract

β1 integrins are important in blood vessel formation and function, finely tuning the adhesion of endothelial cells to each other and to the extracellular matrix. The role of integrins in the vascular disease, cerebral cavernous malformation (CCM) has yet to be explored *in vivo*. Endothelial loss of the gene *KRIT1* leads to brain microvascular defects, resulting in debilitating and often fatal consequences. We tested administration of a monoclonal antibody that enforces the active β1 integrin conformation, (clone 9EG7), on a murine neonatal CCM mouse model, *Krit1*$^{flox/flox}$*;Pdgfb-iCreERT2* (*Krit1*^{ECKO}), and on KRIT1-silenced human umbilical vein endothelial cells (HUVECs). In addition, endothelial deletion of the master regulator of integrin activation, Talin 1 (Tln1), in *Krit1*^{ECKO} mice was performed to assess the effect of completely blocking endothelial integrin activation on CCM. Treatment with 9EG7 reduced lesion burden in the *Krit1*^{ECKO} model and was accompanied by a strong reduction in the phosphorylation of the ROCK substrate, myosin light chain (pMLC), in both retina and brain endothelial cells. Treatment of KRIT1-silenced HUVECs with 9EG7 *in vitro* stabilized cell-cell junctions. Overnight treatment of HUVECs with 9EG7 resulted in significantly reduced total surface expression of β1 integrin, which was associated with reduced pMLC levels, supporting our *in vivo* findings. Genetic blockade of integrin activation by *Tln1*^{ECKO} enhanced bleeding and did not reduce CCM lesion burden in *Krit1*^{ECKO} mice. In sum, targeting β1 integrin with an activated-specific antibody reduces acute murine CCM lesion development, which we found to be associated with suppression of endothelial ROCK activity.

[#]To whom correspondence should be addressed: Sara McCurdy, smccurdy@ucsd.edu, Phone: 858-822-6432.

Author Contributions

S. McCurdy, M.H. Ginsberg, and M. A. Lopez-Ramirez conceived of research aims and created study design; S. McCurdy, J. Lin, R. Shenkar, R. Lightle, and T. Moore performed the research, collected data, and created figures; I. Awad and E. Faurobert contributed intellectually to experimental design and data analysis. All authors were involved in drafting and revising the manuscript.

Conflict of Interest Statement

The authors declare no conflicts of interest.

Introduction

The commonest familial form of cerebral cavernous malformations (CCM) is caused by loss of function mutations in *KRIT1* (also known as *CCM1*). This gene encodes a protein that is a part of a multi-protein complex important in vascular development and stability [1]. CCM patients develop dilated, leaky blood vessels and large, multi-cavernous lesions within the brain, spinal cord, and retina. Chronic and acute bleeding from these lesions results in headaches, seizures, stroke, neurological deficits and occasionally death. Presently, the only specific treatment for CCM is surgical removal of lesions.

Although β1 integrins play essential roles in vascular development and function [2–5], *in vitro* studies have led to apparently conflicting views of the importance of altered integrin function in CCM development following *KRIT1* loss. In particular, integrins can transition to a high affinity state, a process termed integrin activation, resulting from the binding of Talin 1 to the cytoplasmic domain of the integrin β subunit [6, 7]. Integrin cytoplasmic domain-associated protein (ICAP)-1α was discovered as a β1 integrin binding protein that is a competitive inhibitor of Talin 1 binding to the β1 tail [8], thereby suppressing integrin activation. Krev1 interaction trapped 1 (KRIT1) binds to ICAP1-α [9, 10], and biochemical and structural studies led to the idea that KRIT1 sequesters ICAP1-α from β1 integrins, promoting integrin activation [11]. In keeping with this idea, endothelial-specific deletion of β1 integrin [5] or Talin 1 [12] disrupts endothelial cell-cell junctions, a prominent consequence of loss of KRIT1 [13–15]. Additionally, restoration of junctions with a miRNA antagonist that preserves VE-cadherin can suppress CCM formation [16]. Thus, the disruption of cell-cell junctions that follows suppression of β1 integrin activation could contribute to CCM development in KRIT1-deficient endothelial cells (ECs).

A series of studies led to the alternative hypothesis that increased integrin activation following loss of KRIT1 contributes to the development of CCM [17]. In particular, *KRIT1* inactivation results in reduced ICAP1-α expression [18] thereby increasing β1 integrin activation. This results in RhoA/Rho kinase (ROCK) activation with a consequent increase in the phosphorylation of the light chain of myosin II (pMLC) and increased contractility. The combination of integrin activation and increased contractility lead to the expected aberrant fibronectin matrix assembly in *KRIT1*-silenced ECs [17]. Moreover, increased extracellular matrix is a feature of chronic CCM, and ICAP-1 null mice exhibit abnormalities of capillary plexus morphology [17]. Finally, silencing β1 integrin can suppress KLF2 expression in *KRIT1*-silenced human umbilical vein endothelial cells (HUVECs), and a β1b-directed morpholino can suppress the dilated heart phenotype of *ccm*^{201} zebrafish [19]. In another recent study, the ability of KRIT1-deficient ECs to rescue adherens junction and barrier function correlated with decreased β1 integrin activity and suppression of pMLC [32]. In sum, these data make a compelling case for the alternative idea that the increase in integrin activation observed *in vitro* in *KRIT1*-silenced ECs could contribute to the development of CCM.

Here we report that long-term treatment with an antibody that is known to enforce the active conformation of β1 integrin reduces the *in vitro* loss of cell-cell junctions that follows *KRIT1* silencing in ECs, and more importantly, significantly reduces CCM lesion

burden in *Krit1*^{ECKO} mice. In sharp contrast, EC-specific inactivation of Talin 1, which prevents integrin activation [12], did not reduce lesion number and dramatically exacerbated hemorrhage in *Krit1*^{ECKO} mice. Therefore, we propose that the fine-tuning of β1 integrin function by a pharmacological approach could provide a way to limit CCM lesion burden.

Materials and Methods

Cell culture

Human umbilical vein endothelial cells (HUVECs) were obtained from Lonza (C2519A) and cultured in the manufacturer's recommended growth medium and supplement kit (CC-3162). All experiments were performed with cells between passages 5 and 7. HUVECs were passaged 1:3 and seeded into 8-chambered glass slides (Milipore, PEZGS0816) coated with 2μg/mL human fibronectin (Sigma, F2006) for 1 hour at 37°C. For *in vitro* experiments, cells were transfected with 75nM SMARTpool siRNA against *KRIT1* (Dharmacon, M-003825–01) or non-targeting control siRNA (Dharmacon, D-001206–13). Cells were transfected in OptiMEM (Gibco) using lipofectamine3000 (Invitrogen) overnight, and then given fresh growth medium for 48 hours. Cells were equilibrated in reduced serum medium without vascular endothelial growth factor supplement for 2 hours, then treated overnight with 5μg/mL of the following antibodies: 9EG7 (Bio X Cell), AIIB2 (Sigma, MABT409), or IgG isotype control (IgG2a, Bio X Cell, BE0089).

Immunocytochemistry and ImageJ analysis

HUVECs were plated in 6-well plates coated with 2μg/mL fibronectin as described above. Following overnight treatment with 5μg/mL IgG or 9EG7, HUVECs were washed with PBS and fixed in 4% fresh paraformaldehyde for 10 minutes. Immunostaining was performed immediately following blocking with 10% horse serum in 1% BSA/PBS for 30 minutes at room temperature. Primary antibodies against VE-cadherin (R&D, AF938) and zonula occludens (ZO)-1 (ThermoFisher, 61–7300) were diluted in 1% bovine serum albumin (BSA)/PBS and added to the cells overnight at 4°C. Donkey-α-rabbit AlexaFluor 594 (A-21207) and donkey-α-goat AlexaFluor 647 (A-21447) secondary antibodies (both ThermoFisher) were used at a dilution of 1:300 in 1% BSA/PBS and cells were incubated for 1hr at room temperature. Cells were mounted using DAPI-containing mounting medium (Southern Biotech) and allowed to dry overnight before imaging using a Leica SP8 confocal microscope.

For analysis of junctional VE-cadherin and ZO-1 abundance, 5 representative images per treatment group for each of 3 experiments were analyzed. Using the ImageJ line tool, signal intensity along cell borders were measured at equally distributed areas, with a total of 25 measurements across each image, then averaged for comparison across treatment groups.

Western blot

HUVECs were treated with 9EG7 or IgG for 4 hours or overnight (16 hours) as described above. Cells were washed with PBS, then immediately placed on ice and 100 μl lysis buffer (25 mM Tris-HCl, pH 7.6, 150 mM NaCl, 1% Nonidet P-40, 1% sodium deoxycholate, and 0.1% SDS) supplemented with protease and phosphatase inhibitor cocktails (Roche) was

added per well. Total protein was assessed using a Pierce BCA assay (ThermoFisher), and 25 μg protein was loaded per well. A rabbit monoclonal antibody was used to detect total total β1 integrin protein (ThermoFisher, 14–0299-82). Phosphorylated myosin light chain 2 (pMLC) was detected using a Thr18/Ser19 phospho-specific antibody (CST, #3674), while total MLC protein was detected using an MLC pan antibody (CST, #3672). β-actin was used as loading control for all western blot experiments (ThermoFisher, AM4302). Donkey-anti-rabbit (926–32213, LICOR) or goat-anti-mouse (926–68070, LICOR) secondary antibodies were used at 1:10,000 dilution and blots were imaged on a LICOR Odyssey CLX machine.

Flow cytometry

HUVECs were seeded and treated as described for Western blot experiments. After overnight treatment with 9EG7 or IgG, cells were trypsinized and ice-cold culture medium was added before centrifugation at 400 x g for 5 minutes. All antibody staining, washes, and centrifugation steps were performed at 4°C or on ice. After washing with PBS, cells were incubated with Zombie Green live/dead stain (Biolegend) for 20 minutes on ice. Cells were washed with 1% BSA in PBS, then incubated with an APC-conjugated anti-human CD29 antibody against β1 integrin (303008, Biolegend) at a dilution of 1:100 in 1% BSA/PBS for 30 minutes on ice. Cells were washed again and analyzed using an Accuri C6 flow cytometer (BD Biosciences). Live cells were analyzed for APC mean fluorescence intensity (MFI).

Mouse breeding and *in vivo* experimental details

Temporally and spatially controlled deletion of the *Krit1* gene was achieved by crossing C57BL/6 mice with loxP sites flanking exon 5 of the *Krit1* mouse gene ($Krit1^{Flox/Flox}$, a gift from Douglas A. Marchuk, Duke University), and mice with tamoxifen-inducible Cre recombinase driven by the Pdgfb promoter, iCreERT2 [20], to obtain $Krit1^{Flox/Flox}$;*Pdgfb-iCreERT2* mice, referred to throughout the manuscript as $Krit1^{ECKO}$ mice. Postnatal day 1 $Krit1^{ECKO}$ mice were administered 50 μg 4-hydroxy-tamoxifen (Sigma) dissolved in 50 μl corn oil each via intragastric injection to induce endothelial deletion of *Krit1*. At postnatal day 5, Cre-positive neonates were randomly divided into two groups and were administered 4mg/kg of either 9EG7 (rat-α-β1 integrin), or isotype control (rat IgG2a, Bio X Cell, BE0089) antibody in a total volume of 10 μl via retroorbital injection. We decided based on previous experiments from our own lab that between 2 and 10 mg/kg was optimal for use of 9EG7 in adult mice (unpublished). 4mg/kg was chosen as a middle dose that was well-tolerated in preliminary studies. At postnatal day 7, neonates were sacrificed via decapitation, and whole eyes and brains were immediately isolated and kept on ice until fixation. All mouse experiments were performed at the University of California, San Diego in compliance with the Institutional Animal Care and Use Committee.

Preparation and immunohistochemistry of mouse tissue

Eyes were fixed in 2% paraformaldehyde in PBS at 4°C overnight before being washed 3 times with PBS. Retinas were then dissected from surrounding tissue and incubated overnight with blocking buffer (PBS, 1% BSA, and 0.5% Triton X-100). For staining of surface localized 9EG7 antibody, retinas were immediately incubated with donkey-α-rat AlexaFluor 647 secondary antibody at a dilution of 1:300 (ThermoFisher). Retinas were

washed in PBlec buffer (1X PBS, 1mM $CaCl_2$, 1mM $MgCl_2$, 0.1mM $MnCl_2$, 1% Triton X-100) 3X, 5 minutes each, and stained with FITC-conjugated isolectin B_4 (1:80, Sigma-Aldrich) to visualize the vasculature. For staining of pMLC (Cell Signaling Technology, #3674), retinas were blocked as described above, then incubated with pMLC primary antibody (1:50) overnight at room temperature, followed by 48 hours at 4°C. Retinas were washed 5 times with PBS before incubation with donkey-α-rabbit AlexaFluor 647 antibody (1:250, ThermoFisher) for 2 hours at room temp. Retinal whole-mount preparations were washed an additional 5 times with PBS and cut into 4 petals for flat-mounting using Fluoromount-G (SouthernBiotech). Each retina was imaged blindly and a total of 3–5 fields of view at 63x magnification were collected for analysis.

Brains prepared for micro-computed tomography (microCT) were fixed in 10% neutral buffered formalin overnight. Brains were then prepared for microCT scanning as described previously [21]. Briefly, brains were soaked in 1.25% Lugol iodine (ThermoFisher) for 96 h. The Phoenix v|tome|x s 180/240 microCT scanner system (General Electric) was used to acquire images.

Brains isolated for histological analysis were fixed in 4% paraformaldehyde overnight, washed 2X with PBS, embedded in paraffin, and sectioned using a microtome. Brain sections were then deparaffinized, and a citrate unmasking solution was used according to manufacturer's direction (Vector Labs). This was followed by blocking with the Avidin-Biotin blocker kit (#SP-2001, VectorLabs), and incubation of sections with phospho-myosin light chain primary antibody (1:60, Cell Signaling Technology, #3674). Slides were then washed using Tris-buffered saline -Tween and incubated with H_2O_2 to quench endogenous peroxide activity. Incubation with a goat anti-rabbit IgG biotinylated secondary antibody (BP-9100–50, VectorLabs) was followed by development using a DAB kit (SK-4100, VectorLabs). Tissue sections were then counterstained using Hematoxylin QS (H-3404–100, VectorLabs) and dehydrated before mountain and imaging.

Statistics

Throughout the manuscript and figures, all data are expressed as the mean ± SEM of experimental and/or biological replicates. The number of independent experiments (N) or animals within each group (n) is indicated where appropriate throughout the manuscript and in figure legends. Immunostaining analysis of cell samples, brains, and retinas was performed blinded. A standard outlier test was used at the main criteria to determine if any data points should be excluded. No outliers were detected in any data set measured and thus no data points were excluded. Unpaired Student's t-test was used to determine statistical significance between two groups, while one-way ANOVA followed by Tukey's post-hoc test was used for analysis of more than two groups.

Results

Long-term treatment with an anti-activated β1 integrin antibody preserves endothelial cell-cell junctions in *Krit1*-depleted HUVECs

As noted above, disruption of endothelial cell-cell junctions is a prominent consequence of loss of *Krit1* [13, 15]. A monoclonal antibody recognizing the active form of β1 integrin, 9EG7 [22], has been shown previously to stabilize these junctions [12]. We silenced *KRIT1* in HUVECs, reducing mRNA by 83.2±3.7%, and then added 5 μg/ml 9EG7, or an IgG isotype control antibody overnight. *KRIT1*-silenced HUVECs treated with isotype control antibody exhibited reduced junctional ZO-1 and VE-cadherin abundance. These reductions in junctional proteins were partially reversed by overnight treatment with 9EG7 (Figure 1A). Quantification of staining intensity along cell-cell junctions revealed a 42.2±4.3% reduction in junctional VE-cadherin staining in *KRIT1*-silenced cells that was restored to 87.4±6.9% of control in response to 9EG7 (Figure 1B). Western blot analysis revealed no significant differences in total VE-cadherin protein among treatment groups (Supplemental Figure 1), indicating the changes in junctional staining were due to altered localization rather than protein abundance. Similarly, there was a 31±7% reduction in junctional ZO1 staining in *KRIT1*-silenced HUVECs that was restored to 94.4±7% of control in response to 9EG7 (Figure 1C). Importantly, 9EG7 did not affect the efficiency of *KRIT1* silencing, nor did it reverse the elevation of KLF2 and KLF4 expression in these *KRIT1*-silenced HUVECs (Supplemental Figure 2). As an additional control, we examined the effects of a β1 integrin blocking antibody, AIIB2 [23]. Unlike the stabilizing effects seen with 9EG7 treatment, treatment with the AIIB2 antibody failed to rescue VE-cadherin or ZO-1 junctional abundance (Supplemental Figure 3A, quantified in panels B and C respectively). Taken together, these data indicate that β1 integrin targeting with 9EG7 specifically can oppose the effects of silencing *KRIT1* on endothelial cell-cell junctions.

To gain further insight into the molecular effect of long-term treatment with 9EG7 on β1 integrin function, we assessed surface levels of β1 integrin in HUVECs using flow cytometry. Overnight treatment with 9EG7 halved the surface expression of β1 integrin compared to untreated or IgG controls (Figure 2A); however, there was no significant difference in total β1 integrin protein abundance (Figure 2B), suggesting that 9EG7 affected activated β1 integrin trafficking without altering stability. 9EG7 treatment of HUVECs has been shown previously to ameliorate the junction defect in *Tln1*-silenced HUVECs [12]. Additionally, the knock-down of β1 integrin has been shown to block the activation of RhoA/ROCK and the formation of actin stress fibers in KRIT1- and CCM2-silenced HUVECs [18]. Since inhibition of ROCK can reduce the effects of loss of KRIT1 on endothelial cell (EC) junctional stability [24], we thus measured the effect of 9EG7 treatment on pMLC levels in quiescent control cells (Figure 2C), as well as *KRIT1*-silenced HUVECs (Figure 2D). We observed that the level of pMLC was significantly reduced in 9EG7-treated HUVECs compared to IgG control-treated cells in both conditions. Importantly, 9EG7 treatment of *Krit1*-silenced HUVECs led to a striking reduction of pMLC to a level equivalent to scrambled control siRNA-treated HUVECs (siScr) (Figure 2D). Thus, 9EG7 can reverse the effect of KRIT1 deficiency on endothelial cell-cell junctions associated with reduced ROCK activity and surface β1 integrin expression.

Treatment with 9EG7 ameliorates murine CCM

Previous studies showed a strong correlation between treatments that preserve endothelial cell-cell junctions and amelioration of CCM, leading us to test the effects of 9EG7 in a *Krit1* EC knock out (*Krit1*^{ECKO}) acute neonatal mouse model of CCM disease [15]. Endothelial-specific deletion of *Krit1* was induced in *Krit1*$^{flox/flox}$;*Pdgfb-iCreERT2* neonatal mice (hereafter referred to as *Krit1*^{ECKO}) by administering 50μg of 4-hydroxy-tamoxifen via intragastric injection on postnatal day 1. Postnatal day 5 mice were administered 4mg/kg 9EG7 or IgG isotype control antibody by retro-orbital injection. The mice were then sacrificed, and retinas and brains were collected at postnatal day 7 for further analysis (Fig. 3A). Brains were analyzed by micro-computed tomography (microCT) for total lesion volume or sectioned for histological analysis. To confirm delivery of the antibodies to the central nervous system, retinas were isolated and stained with an Alexa Flour 647-conjugated anti-rat IgG to detect 9EG7 or isotype control antibodies. 9EG7 was detected as magenta pseudocolor staining in retinas (Supplemental Figure 4), whereas there was no detectable signal in isotype IgG or phosphate buffered saline (PBS)-injected control retinas. 9EG7 treatment resulted in a dramatic reduction in lesion burden in *Krit1*^{ECKO} mice as assessed by microCT (Figure 3B,C). Hindbrain sections stained with hematoxylin and eosin (Figure 3D) revealed a significant reduction in the average size of individual lesions and a trend towards reduced lesion number in 9EG7-treated mice compared to IgG-treated controls (Figure 3E,F). Thus, 9EG7 reduced CCM burden in the *Krit1*^{ECKO} acute mouse model.

9EG7 suppresses endothelial myosin light chain phosphorylation in *Krit1*^{ECKO} mice

The activation of ROCK is known to contribute to compromised endothelial cell-cell junctions [24], and the development of CCM following loss of KRIT1 [25]. As noted above, our *in vitro* experiments have shown that 9EG7 can prevent junction defects (Figure 1) and suppress ROCK activity as measured by reduced pMLC level (Figure 2) *in vitro*. Similarly, 9EG7 treatment significantly reduced pMLC staining in retinal (Figure 4A, B) and CCM lesion ECs (Figure 4C, D). Thus, the protective effects of 9EG7 antibody treatment on CCM, observed both *in vitro* and *in vivo*, is associated with inhibition of ROCK.

Genetic inhibition of integrin activation does not reduce CCM lesion number

To test the effect of genetic inhibition of integrin activation, we crossed *Tln1*$^{fl/fl}$ and *Krit1*$^{fl/fl}$ *Pdgfb-iCreERT2 mice and intercrossed the offspring to produce Tln1*$^{fl/fl}$;*Krit1*$^{fl/fl}$;*Pdgfb-iCreERT2 (Tln1/Krit1*^{ECKO}) mice and *Tln1*$^{+/+}$;*Krit1*$^{fl/fl}$;*Pdgfb-iCreERT2 (Krit1*^{ECKO}) controls. Since Talin 1 is required for integrin activation, we analyzed the effect of post-natal deletion of endothelial *Tln1* on CCM lesion development. We found that inactivation of *Tln1* failed to reduce the CCM lesions caused by loss of *Krit1* (Figure 5). *Tln1/Krit1*^{ECKO} animals showed substantial microhemorrhage throughout the brain, visualized by microCT (Figure 5A,B) and histological analysis (Figure 5C, hollow arrows). CD31 staining revealed that the number of CCM lesions (Figure 5C, solid arrows) was not reduced by Talin 1 deletion, indicating that genetic blockade of integrin activation *in vivo* is not protective in this model of CCM disease.

Discussion

β1 integrins are present at both cell-cell and cell-matrix junctions in ECs and play important roles in vascular development, physiology, and pathology. Genetic endothelial depletion of β1 integrin or of Talin 1, its master activator, both perturb VE-cadherin localization at cell-cell junctions and compromise vascular integrity [5, 13]. Similarly, genetic depletion of ICAP1-α, a negative regulator of β1 integrin activation [9], also leads to defective VE-cadherin–dependent cell-cell junctions and increased vascular permeability [18]. Therefore, it is likely that a finely tuned level of activated β1 integrin is required at the cell surface to allow the formation of barrier competent cell-cell junctions.

KRIT1 is the first gene whose loss of function was identified as a cause of familial CCM [26, 27]. The discovery of the binding of KRIT1 to ICAP1-α led to elegant structural and cell biological studies to test the role of β1 integrin in CCM defects *in vitro* [28]. Here, we employed the neonatal $Krit1^{ECKO}$ CCM mouse model to examine this question *in vivo.* Administration of the monoclonal antibody 9EG7, recognizing activated β1 integrin, reduced CCM lesion burden by 55±10%. Because acute CCM disease is driven mainly by endothelial dysfunction, we assessed the effects of this antibody on HUVECs *in vitro.* Loss of cell-cell junctions is an early consequence of loss of *KRIT1* function [13–15], and this was largely reversed by treating *KRIT1*-silenced HUVECs overnight with 9EG7. Suppression of ROCK has been shown to reduce the junctional defect in *KRIT1*-silenced HUVECs [24] and ameliorate CCM burden in a murine model [25]. Accordingly, *in vivo* administration of 9EG7 reduced ROCK-dependent phosphorylation of myosin light chain in ECs of $Krit^{ECKO}$ mice, providing a cogent mechanism for the effect of the 9EG7 on CCM formation.

The 9EG7 antibody enforces the extended open conformation of β1 integrin [29]. Additionally, Pulous et al. reported that treatment of HUVECs with 9EG7 strengthened junctions and increased barrier integrity after loss of Talin1, supporting an important role for activated β1 integrin in maintaining endothelial junctions [12]. We previously reported that KRIT1 silencing activates Rho kinase and disrupts endothelial cell-cell junctions and that blocking this enzyme can both restore the junctions and prevent CCM [24, 25]. Here we report that 9EG7 reverses both the increased Rho kinase activity and disrupted endothelial cell-cell junctions in KRIT1 silenced HUVECs (Figures 1, 2, & 4). Thus, reduced Rho kinase activity provides one explanation for the capacity of 9EG7 to ameliorate the CCM in $Krit1^{ECKO}$ mice (Supplemental Figure 5, left panel).

Importantly, we observed that 9EG7 treatment down-regulated the surface β1 integrin level in HUVECs, without a reduction in total β1 integrin (Supp. Fig. 1). This could account for part of 9EG7's protective effect *in vivo* via reduced ROCK activity (Supplemental Figure 5, right panel). Additionally, it is possible that the interaction of 9EG7 with activated β1 integrin alters its endocytic trafficking, which has previously been shown to regulate RhoA/ROCK activation [30]. We also tested the effect of complete blockade of integrin activation by deleting Talin 1 in ECs of $Krit1^{ECKO}$ mice [12] and observed no reduction in CCM lesion number. Neonatal deletion of endothelial Talin 1 led to dramatically enhanced bleeding in these mice, supporting the central role of integrin function in the maintenance of endothelial

cell-cell junctions and overall vascular integrity [5]. Thus, contrary to genetic approaches, our pharmacological treatment with 9EG7 proved to be efficient in maintaining a beneficial surface level of activated β1 integrin at which cell-cell junctions were preserved and RhoA/ROCK activity was limited.

The complexity of the crosstalk between integrin-mediated adhesion, blood flow, and adherens junctions raises other interesting avenues for future research. For example, deletion of β1 integrins can reduce the endothelial response to blood flow [31], and aberrantly increased flow sensing is a prominent feature of vasculature response to the loss of KRIT1 [19, 32, 33]. KRIT1 deficiency causes disrupted endothelial apical basal polarity, possibly secondary to disrupted adherens junctions [14], a defect also seen upon total endothelial loss of β1 integrins [34]. Thus, an antibody that fine tunes activation of β1 integrins, by stabilizing those junctions, may help reduce this polarity defect. We also note that the acute neonatal model used here reflects the acute process of CCM formation; whereas in humans, lesions are usually more chronic and suffer sequelae such as recurrent bleeding and inflammation present in more chronic murine models [35–38]. Because 9EG7 is of rat origin, the generation of mouse anti-rat antibodies precluded experiments to test the effects of 9EG7 in chronic CCM models. In sum, a monoclonal antibody that targets activated β1 integrin reduces CCM lesion burden in an acute murine $Krit1^{ECKO}$ model in association with a reduction in ROCK activity and stabilization of endothelial cell-cell junctions, indicating that a finely tuned level of activated β1 integrin on the cell surface can ameliorate lesion burden in this murine CCM model.

Supplementary Material

Refer to Web version on PubMed Central for supplementary material.

Acknowledgments

The authors thank Chin Chu Lai and Wilma McLaughlin and for technical assistance, as well as Jennifer Santini for microscopy technical assistance. We also thank Olivier Destaing for helpful discussion.

Sources of Funding

This work was supported by the National Institutes of Health, National Institute of Neurological Disorder and Stroke grant P01HL151433 (M.H.G., M.A.L.-R.); the National Heart, Lung, and Blood Institute grants NS092521 (M.H.G.) and 5T32HL086344 (M.H.G.); and Microscopy Core grant P30 NS047101.

Data Availability Statement

The data that support the findings of this study are available in the main text, figures, and/or supplemental data of the manuscript.

References

1. Maddaluno L, et al. , EndMT contributes to the onset and progression of cerebral cavernous malformations. Nature, 2013. 498(7455): p. 492–6. [PubMed: 23748444]
2. Lei L, et al. , Endothelial expression of beta1 integrin is required for embryonic vascular patterning and postnatal vascular remodeling. Mol Cell Biol, 2008. 28(2): p. 794–802. [PubMed: 17984225]

3. Tanjore H, et al. , Beta1 integrin expression on endothelial cells is required for angiogenesis but not for vasculogenesis. Dev Dyn, 2008. 237(1): p. 75–82. [PubMed: 18058911]
4. Carlson TR, et al. , Cell-autonomous requirement for beta1 integrin in endothelial cell adhesion, migration and survival during angiogenesis in mice. Development, 2008. 135(12): p. 2193–202. [PubMed: 18480158]
5. Yamamoto H, et al. , Integrin beta1 controls VE-cadherin localization and blood vessel stability. Nat Commun, 2015. 6: p. 6429. [PubMed: 25752958]
6. Ye F, et al. , Recreation of the terminal events in physiological integrin activation. J Cell Biol, 2010. 188(1): p. 157–73. [PubMed: 20048261]
7. Shattil SJ, Kim C, and Ginsberg MH, The final steps of integrin activation: the end game. Nat Rev Mol Cell Biol, 2010. 11(4): p. 288–300. [PubMed: 20308986]
8. Bouvard D, et al. , Disruption of focal adhesions by integrin cytoplasmic domain-associated protein-1 alpha. J Biol Chem, 2003. 278(8): p. 6567–74. [PubMed: 12473654]
9. Zawistowski JS, et al. , KRIT1 association with the integrin-binding protein ICAP-1: a new direction in the elucidation of cerebral cavernous malformations (CCM1) pathogenesis. Hum Mol Genet, 2002. 11(4): p. 389–96. [PubMed: 11854171]
10. Zhang J, et al. , Interaction between krit1 and icap1alpha infers perturbation of integrin beta1-mediated angiogenesis in the pathogenesis of cerebral cavernous malformation. Hum Mol Genet, 2001. 10(25): p. 2953–60. [PubMed: 11741838]
11. Draheim KM, et al. , Nuclear Localization of Integrin Cytoplasmic Domain-associated Protein-1 (ICAP1) Influences beta1 Integrin Activation and Recruits Krev/Interaction Trapped-1 (KRIT1) to the Nucleus. J Biol Chem, 2017. 292(5): p. 1884–1898. [PubMed: 28003363]
12. Pulous FE, et al. , Talin-Dependent Integrin Activation Regulates VE-Cadherin Localization and Endothelial Cell Barrier Function. Circ Res, 2019. 124(6): p. 891–903. [PubMed: 30707047]
13. Glading A, et al. , KRIT-1/CCM1 is a Rap1 effector that regulates endothelial cell cell junctions. J Cell Biol, 2007. 179(2): p. 247–54. [PubMed: 17954608]
14. Lampugnani MG, et al. , CCM1 regulates vascular-lumen organization by inducing endothelial polarity. J Cell Sci, 2010. 123(Pt 7): p. 1073–80. [PubMed: 20332120]
15. Lopez-Ramirez MA, et al. , Thrombospondin1 (TSP1) replacement prevents cerebral cavernous malformations. J Exp Med, 2017. 214(11): p. 3331–3346. [PubMed: 28970240]
16. Li J, et al. , Targeting miR-27a/VE-cadherin interactions rescues cerebral cavernous malformations in mice. PLoS Biol, 2020. 18(6): p. e3000734. [PubMed: 32502201]
17. Faurobert E, et al. , CCM1-ICAP-1 complex controls beta1 integrin-dependent endothelial contractility and fibronectin remodeling. J Cell Biol, 2013. 202(3): p. 545–61. [PubMed: 23918940]
18. Zhang J, et al. , Krit1 modulates beta 1-integrin-mediated endothelial cell proliferation. Neurosurgery, 2008. 63(3): p. 571–8; discussion 578. [PubMed: 18812969]
19. Renz M, et al. , Regulation of beta1 integrin-Klf2-mediated angiogenesis by CCM proteins. Dev Cell, 2015. 32(2): p. 181–90. [PubMed: 25625207]
20. Claxton S, et al. , Efficient, inducible Cre-recombinase activation in vascular endothelium. Genesis, 2008. 46(2): p. 74–80. [PubMed: 18257043]
21. Girard R, et al. , Micro-computed tomography in murine models of cerebral cavernous malformations as a paradigm for brain disease. J Neurosci Methods, 2016. 271: p. 14–24. [PubMed: 27345427]
22. Bazzoni G, et al. , Monoclonal antibody 9EG7 defines a novel beta 1 integrin epitope induced by soluble ligand and manganese, but inhibited by calcium. J Biol Chem, 1995. 270(43): p. 25570–7. [PubMed: 7592728]
23. Takada Y and Puzon W, Identification of a regulatory region of integrin beta 1 subunit using activating and inhibiting antibodies. J Biol Chem, 1993. 268(23): p. 17597–601. [PubMed: 7688727]
24. Stockton RA, et al. , Cerebral cavernous malformations proteins inhibit Rho kinase to stabilize vascular integrity. J Exp Med, 2010. 207(4): p. 881–96. [PubMed: 20308363]

25. McDonald DA, et al. , Fasudil decreases lesion burden in a murine model of cerebral cavernous malformation disease. Stroke, 2012. 43(2): p. 571–4. [PubMed: 22034008]
26. Sahoo T, et al. , Mutations in the gene encoding KRIT1, a Krev-1/rap1a binding protein, cause cerebral cavernous malformations (CCM1). Human Molecular Genetics, 1999. 8(12): p. 2325–33. [PubMed: 10545614]
27. Laberge-le Couteulx S, et al. , Truncating mutations in CCM1, encoding KRIT1, cause hereditary cavernous angiomas. Nat Genet., 1999. 23(2): p. 189–93. [PubMed: 10508515]
28. Liu W, et al. , Mechanism for KRIT1 release of ICAP1-mediated suppression of integrin activation. Mol Cell, 2013. 49(4): p. 719–29. [PubMed: 23317506]
29. Su Y, et al. , Relating conformation to function in integrin alpha5beta1. Proc Natl Acad Sci U S A, 2016. 113(27): p. E3872–81. [PubMed: 27317747]
30. Jacquemet G, et al. , RCP-driven alpha5beta1 recycling suppresses Rac and promotes RhoA activity via the RacGAP1-IQGAP1 complex. J Cell Biol, 2013. 202(6): p. 917–35. [PubMed: 24019536]
31. Xanthis I, et al. , beta1 integrin is a sensor of blood flow direction. J Cell Sci, 2019. 132(11).
32. Li J, et al. , Low fluid shear stress conditions contribute to activation of cerebral cavernous malformation signalling pathways. Biochim Biophys Acta Mol Basis Dis, 2019. 1865(11): p. 165519. [PubMed: 31369819]
33. Macek Jilkova Z, et al. , CCM proteins control endothelial beta1 integrin dependent response to shear stress. Biol Open, 2014. 3(12): p. 1228–35. [PubMed: 25432514]
34. Zovein AC, et al. , Beta1 integrin establishes endothelial cell polarity and arteriolar lumen formation via a Par3-dependent mechanism. Dev Cell, 2010. 18(1): p. 39–51. [PubMed: 20152176]
35. Zeineddine HA, et al. , Phenotypic characterization of murine models of cerebral cavernous malformations. Lab Invest, 2019. 99(3): p. 319–330. [PubMed: 29946133]
36. Plummer NW, et al. , Loss of p53 sensitizes mice with a mutation in Ccm1 (KRIT1) to development of cerebral vascular malformations. Am J Pathol, 2004. 165(5): p. 1509–18. [PubMed: 15509522]
37. Detter MR, et al. , Novel Murine Models of Cerebral Cavernous Malformations. Angiogenesis, 2020. 23(4): p. 651–666. [PubMed: 32710309]
38. Cardoso C, et al. , Novel Chronic Mouse Model of Cerebral Cavernous Malformations. Stroke, 2020. 51(4): p. 1272–1278. [PubMed: 31992178]

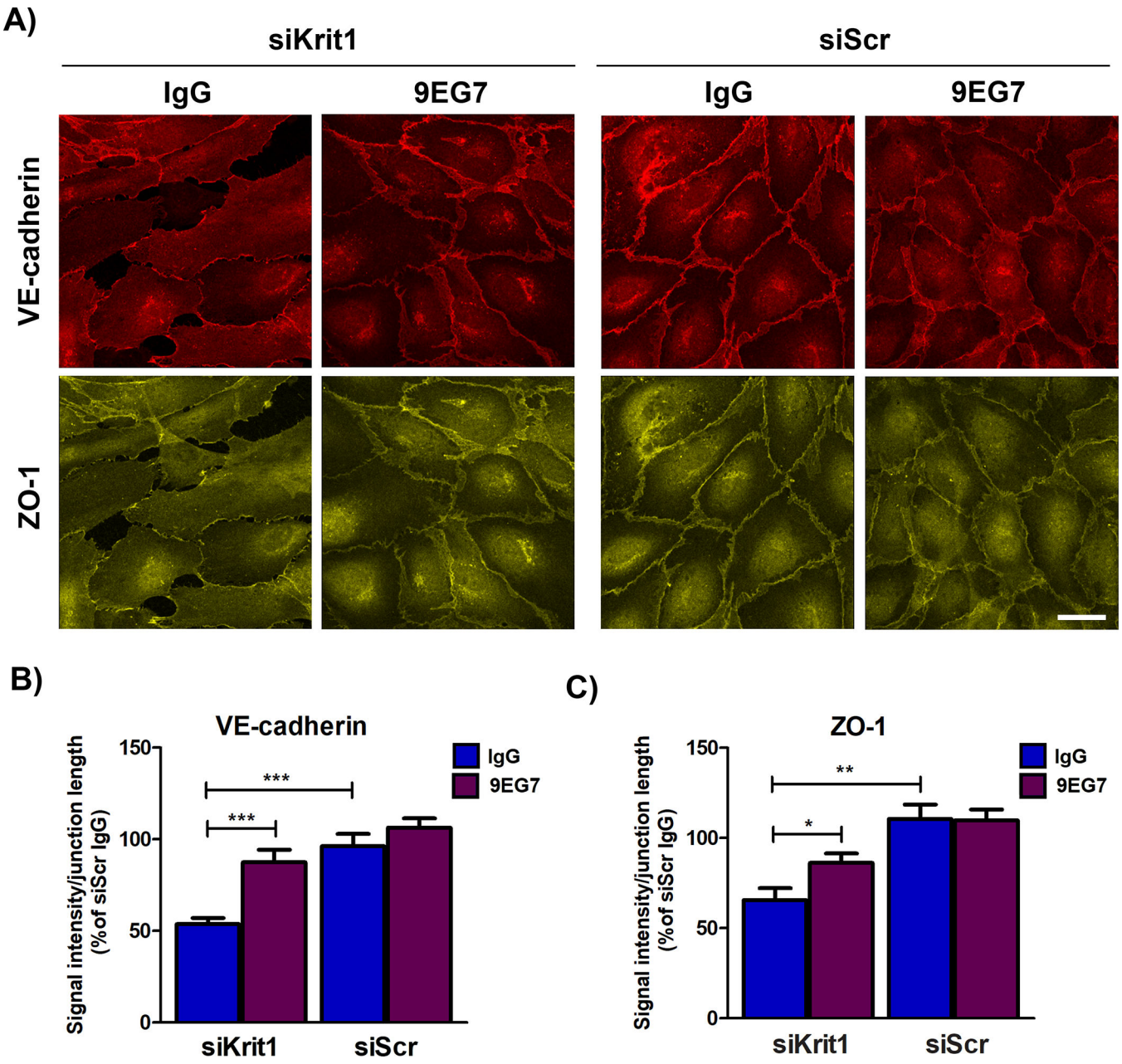

Figure 1. Long-term (overnight) treatment with 9EG7 antibody preserves endothelial cell-cell junctions in *Krit1*-silenced endothelial cells.

HUVECs, grown on fibronectin-coated glass chambered slides, were transfected with *KRIT1* (siKrit1) or scrambled control (siScr) siRNA for 48 hours. **(A)** The cells were treated overnight with 5 μg/mL 9EG7 or IgG isotype control antibody before they were fixed and stained for junctional proteins, VE-cadherin or zonula occludens (ZO)-1. **(B,C)** Staining intensity was measured along cell-cell junctions using ImageJ and is reported as a percent of IgG-treated, siRNA-transfected control. Silencing *KRIT1* resulted in decreased VE-cadherin and ZO-1 abundance along cell-cell junctions (57.8±4.3% and 69±7% of control levels respectively). Treatment with 9EG7 rescued VE-cadherin and ZO-1 levels to 87.4±6.9%

and 94.4±7% of control levels, respectively. (Scale bar 25 nm., one-way ANOVA, *p<0.05, **p<0.01, ***p<0.001, N=4)

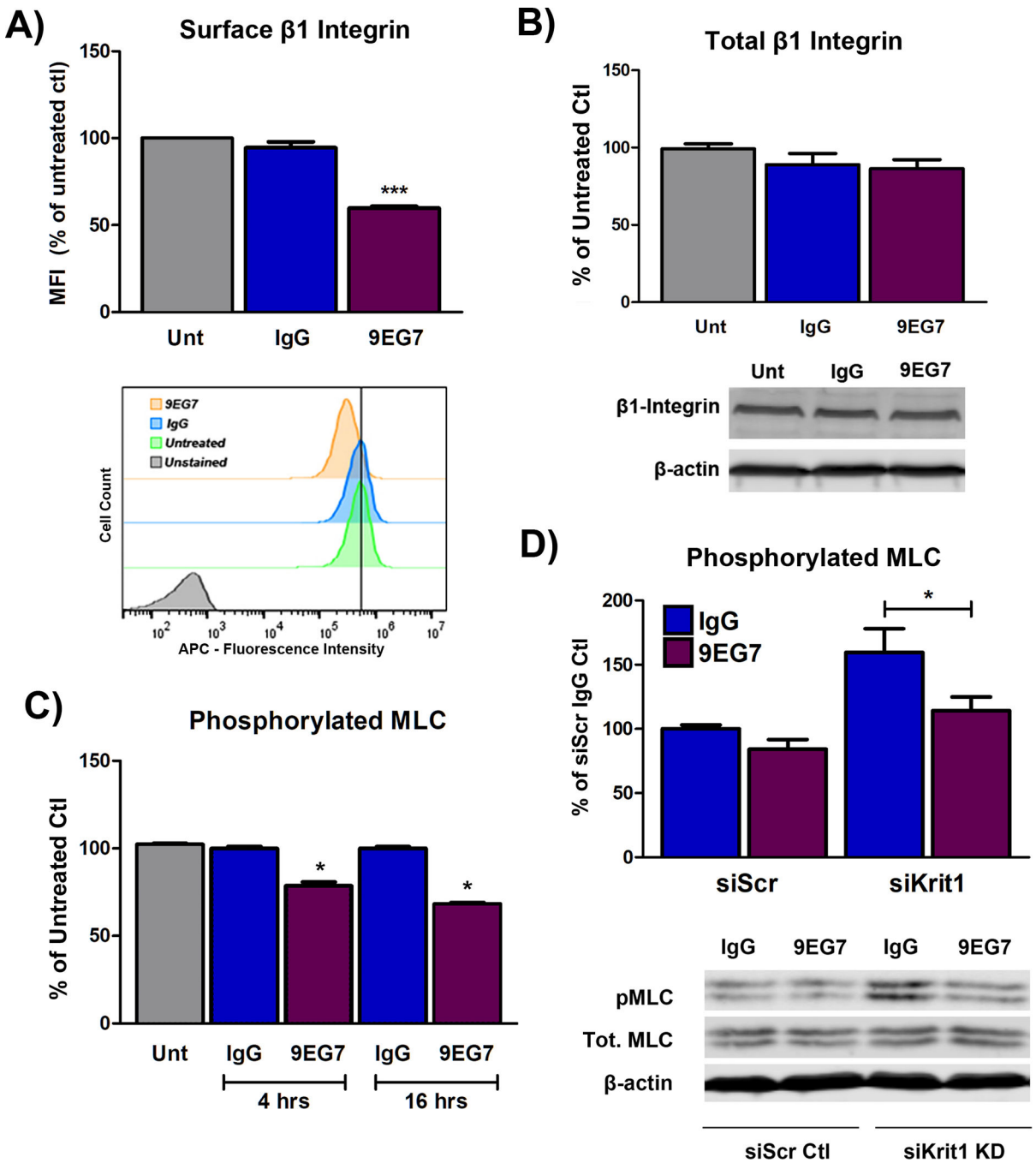

Figure 2. Long-term (overnight) 9EG7 antibody treatment leads to downregulation of surface β1 integrin and reduced pMLC.

(A) HUVECs were treated overnight with either IgG isotype control or 9EG7 antibody at a concentration of 5 μg/mL, or left untreated (Unt). Cells were trypsinized and stained on ice using an APC-conjugated anti-β1 integrin (clone TS2/16) antibody to assess surface β1 integrin levels by flow cytometry. (N=4). Mean fluorescence intensity (MFI) for each condition is represented as a percent of untreated control (ctl). **(B)** HUVECs were treated with 9EG7 or IgG as described above. Cells were lysed in RIPA buffer and total β1 integrin

was analyzed by Western blot, with no significant differences observed between samples (N=3). **(C)** HUVEC lysates were analyzed by Western blot for phosphorylated myosin light chain (pMLC) and total MLC. β-actin was used as loading control. (N=5) **(D)** HUVECs were transfected with scrambled control (siScr Ctl) or *KRIT1*-targeting (siKrit1 KD) siRNA for 48 hours before overnight treatment with IgG or 9EG7 as described above. Silencing *KRIT1* resulted in increased pMLC levels in IgG-treated cells, while treatment with 9EG7 significantly reduced pMLC levels in *Krit1*-silenced cells.(N=4) (*p<0.05, ***p<0.001).

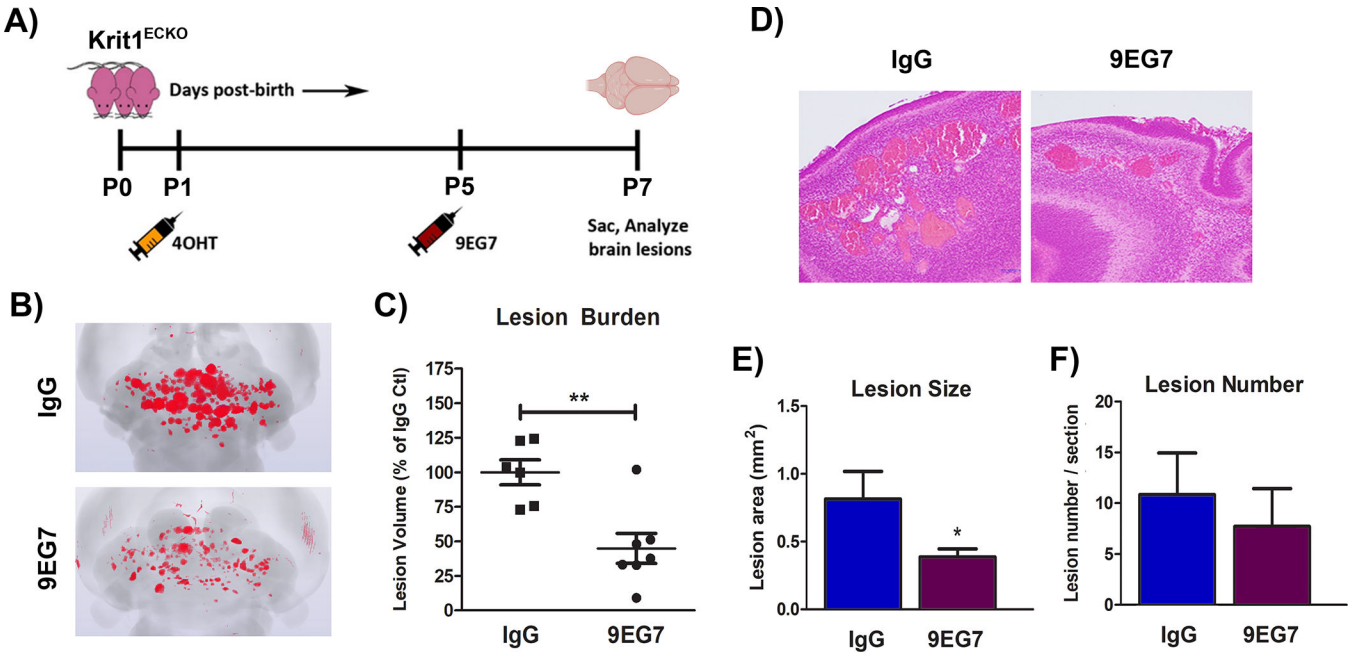

Figure 3. ***In vivo*** **treatment with 9EG7 ameliorates cerebral cavernous malformations.**

Schematic of treatment timeline is shown **(A).** Postnatal day 1 (P1) mice were administered 50μg 4-hydroxy-tamoxifen to induce deletion of *Krit1*. Following genotyping, *Krit1*^{ECKO} mice were divided into two groups and were administered 4mg/kg 9EG7 (n=7) or IgG isotype control (IgG Ctl, n=6) antibody via retroorbital injection at postnatal day 5 (P5). At postnatal day 7 (P7), the mice were sacrificed and brains were collected for analysis by micro-computed tomography **(B,C)** or histologically with H&E staining **(D-F)**. Total lesion volume **(C)**, and average lesion size **(E)**, were significantly reduced in 9EG7-treated mice, while lesion number **(F)** was not significantly changed. (Student's t-test, *p<0.05, **p<0.01)

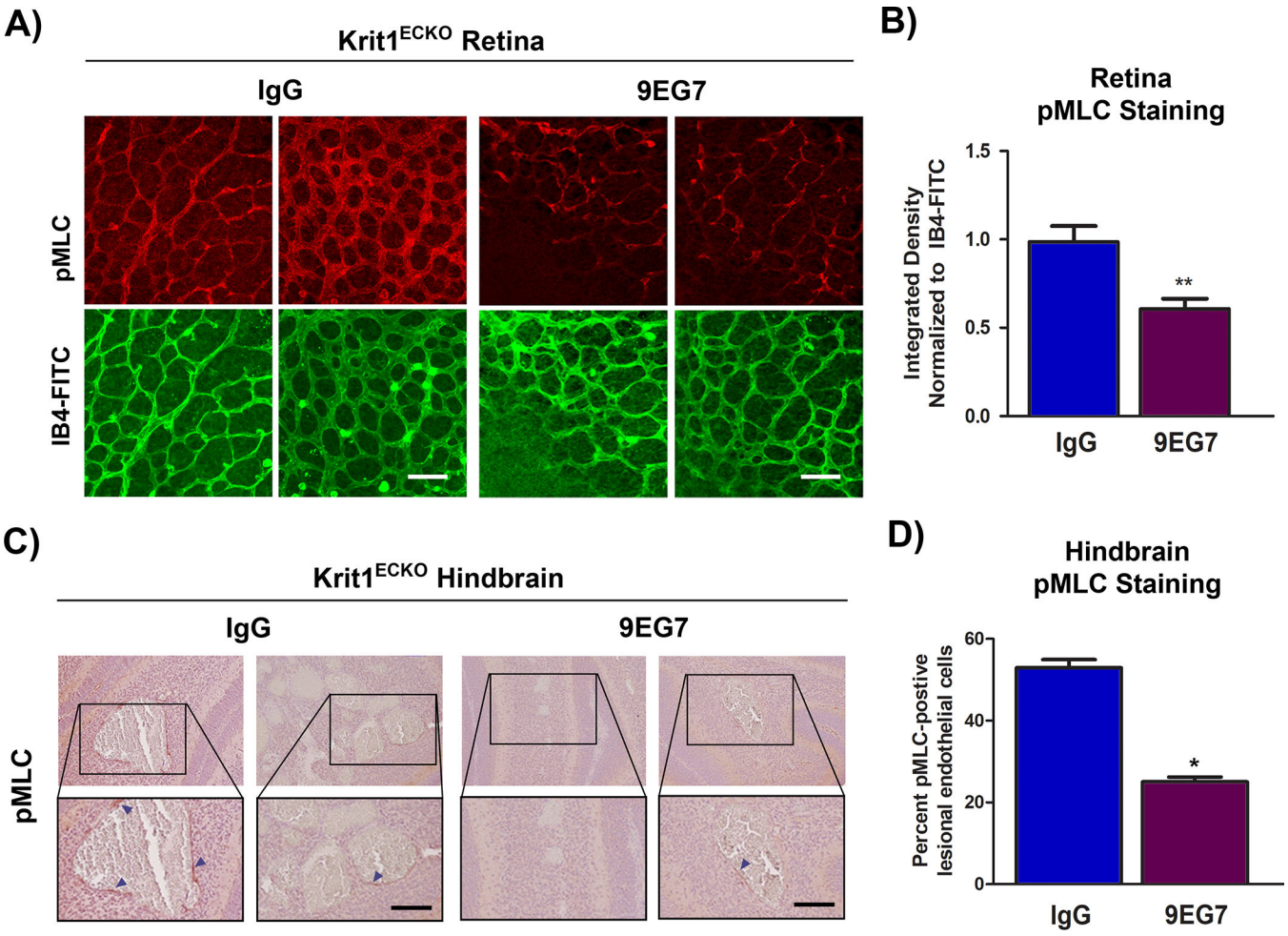

Figure 4. Administration of 9EG7 antibody suppresses myosin light chain phosphorylation in *Krit1*^{ECKO} mice.

Retinas and sectioned hindbrain tissue from 9EG7 or control IgG-treated *Krit1*^{ECKO} mice (treated as previously described in Figure 3A) were immunostained for phosphorylated-myosin light chain (pMLC). pMLC staining in retinal tissue was normalized to isolectin B_4 (IB4-FITC) and expressed as a percent of IgG control **(A,B)** (n=4). pMLC-positive endothelial cells within CCM lesions were detected in hindbrain sections and quantified as a percent of total endothelial cells within the lesion **(C,D)** (n=3). β1-integrin activation *in vivo* had a suppressive effect on pMLC levels in both retina and brain samples. (Scale bar (A): 50μm, (C): 75 μm. *p<0.05, **p<0.01).

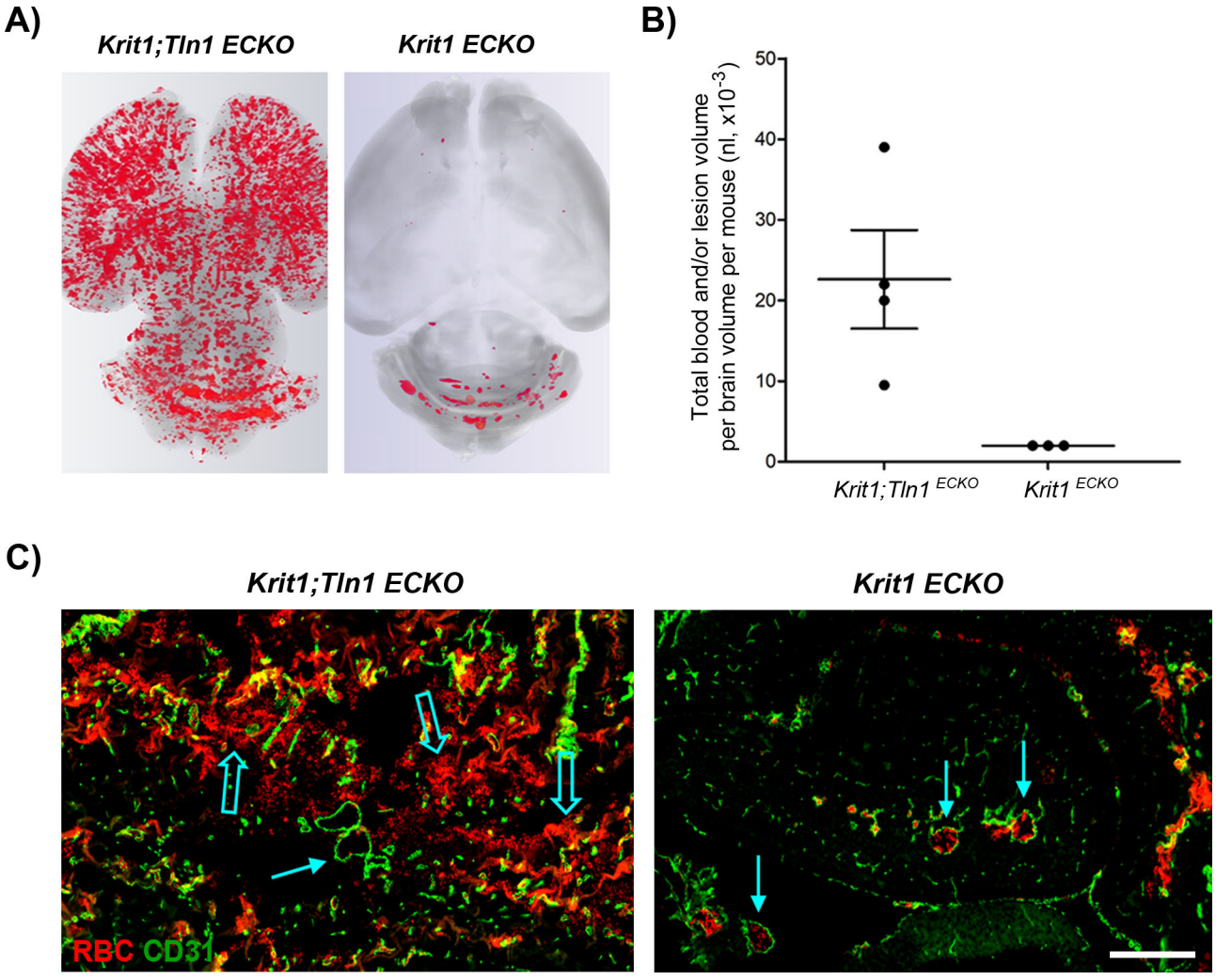

Figure 5. Endothelial loss of Talin1 does not rescue CCM1 lesions caused by *Krit1*^{ECKO}.

Postnatal day 1 mice were administered 50μg 4-hydroxy-tamoxifen to induce deletion of *Krit1* and *Tln1* (n=4), or *Krit1* alone (n=3). At postnatal day 7, the mice were sacrificed and brains were collected for analysis by micro-computed tomography **(A,B).** Hindbrains were also cryosectioned and analyzed by immunofluorescent staining for CD31 (green) or red blood cells (red) **(C)**. CCM lesions are indicated by solid teal arrows, while micro-hemorrhage, abundant in *Krit1;Tln1*^{ECKO} mice, is indicated by hollow teal arrows **(C)**. (Scale bar: 100μm)